Biochemical Pharmacology, Vol. 40, No. 9, pp. 1981–1988, 1990.
Printed in Great Britain.

0006-2952/90 $3.00 + 0.00

CYTOTOXIC SYNERGISM BETWEEN TRIMETREXATE AND ETOPOSIDE

EVIDENCE THAT TRIMETREXATE POTENTIATES ETOPOSIDE-INDUCED PROTEIN-ASSOCIATED DNA STRAND BREAKS IN L1210 LEUKEMIA CELLS THROUGH ALTERATIONS IN INTRACELLULAR ATP CONCENTRATIONS

DAVID W. FRY*
Pharmaceutical Research Division, Warner-Lambert Co., Ann Arbor, MI 48105, U.S.A.

(*Received* 7 *December* 1989; *accepted* 8 *May* 1990)

Abstract—Using an outgrowth method, combinations of trimetrexate and etoposide were synergistic against L1210 leukemia as assessed by the median-effect method. Trimetrexate was also found to stimulate etoposide-mediated protein-associated DNA strand breaks by nearly 2-fold when L1210 cells were exposed to 0.5 μM drug(s) for 2 hr. Trimetrexate had no effect on the transport of etoposide or the repair of etoposide-induced DNA strand breaks. Other drugs that interfere with *de novo* purine biosynthesis, including methotrexate and 5,10-dideazatetrahydrofolate, also potentiated etoposide-induced DNA strand breaks, whereas agents that specifically reduce intracellular concentrations of pyrimidines (pyrazofurin or CB-3717) had no effect. Only those protectants that restored ATP levels (adenosine or hypoxanthine) could abolish the stimulatory effect of trimetrexate. Finally, it was shown that by exposing cells to various concentrations of 2,4-dinitrophenol, there was an inverse relationship between the number of DNA strand breaks produced by etoposide and the intracellular concentrations of ATP down to about 600 μM. The results indicate that trimetrexate stimulates etoposide-induced DNA strand breaks possibly by modulating intracellular ATP levels which may contribute to the synergistic interaction between these drugs.

Although the potential success of any new anticancer agent depends heavily on the demonstration of a broad spectrum and a high degree of activity as a single agent, most new drugs are incorporated eventually into clinical regimens involving combinations of two or more drugs. The reasons that combination chemotherapy is usually more advantageous can involve a number of factors including acquired resistance to specific single agents, tumor heterogeneity, severe dose-limiting toxicity, or therapeutic synergy between drugs. Synergism has been observed between a number of drugs and several reasons for these interactions have been proposed which include circumvention of resistance to one drug by another, non-overlapping host toxicities, kinetic effects on cell cycle distribution or biochemical modulation.

The present study describes the biochemical interactions between trimetrexate and etoposide which are relatively new drugs currently used in the clinic and mechanistically quite distinct. Trimetrexate [5 - methyl - 6 - [[(3,4,5 - trimethoxyphenyl)amino]-methyl]-2,4-quinazolinediamine] is a "nonclassical" antifolate (i.e. does not possess a glutamate moiety) and is one of a series of 2,4-diaminoquinazolines [1, 2]. This compound, currently undergoing clinical trial, is a potent inhibitor of dihydrofolate reductase and exhibits a broad spectrum of activity against a variety of murine tumor models, many of which are refractory to methotrexate [3, 4].

Etoposide is a semisynthetic derivative of podophyllotoxin with a respectable spectrum of activity [5, 6] especially against testicular [7] and small cell lung carcinoma [8]. This drug causes a dose-dependent production of protein-associated DNA strand breaks mediated by topoisomerase II. These and other pharmacological aspects of etoposide are reviewed in Ref. 9.

This paper describes a cytotoxic synergy in L1210 leukemia exposed to combinations of trimetrexate and etoposide and provides evidence to suggest a specific biochemical mechanism for this phenomenon.

METHODS

Chemicals. Trimetrexate glucuronate was obtained from Parke–Davis Pharmaceutical Research Division (Ann Arbor, MI). Pyrazofurin and 5,10-dideazatetrahydrofolate were gifts from Eli Lilly & Co. (Indianapolis, IN). Etoposide was a gift from the Bristol-Myers Co. (Syracuse, NY). 2,4-Dinitrophenol was from the Sigma Chemical Co. (St. Louis, MO), and [^{3}H]etoposide was from Moravek (City of Industry, CA).

Cell culture. All experiments employed L1210 mouse leukemia cells grown as a suspension culture in RPMI 1640 medium (Gibco Laboratories)

* Correspondence: Dr. David W. Fry, Pharmaceutical Research Division, Warner-Lambert Co., 2800 Plymouth Rd., Ann Arbor, MI 48105.

supplemented with 10% fetal bovine serum and 50 μg/mL gentamycin. During all drug treatments, cells were in early log growth at a density of approximately 2×10^5/mL. The doubling time was 12–13 hr, and viability was greater than 95% as measured by trypan blue exclusion. Outgrowth experiments involved exposing the cells to drug(s) for 2 hr, washing the cells twice in warmed medium, and reseeding as described above. Intracellular water was determined by the method of Rottenberg [10] using tritiated H_2O to determine total water and [^{14}C]inulin as a measure of the extracellular space.

Analysis of combined drug effects. Results from the above outgrowth experiments were analyzed using the median–effect principle described by Chou and Talalay [11, 12]. Unlike the fractional product and isobologram methods, the median–effect methods allows analysis of combined drug effects independent of individual drug kinetics or mechanism of drug action. In its simplest form, the median–effect equation depicts the equality of two dimensionless ratios:

$$\frac{f_a}{f_u} = \left[\frac{D}{D_m}\right]^m \tag{1}$$

where D is the dose; f_a and f_u are the fractions of the system affected and unaffected, respectively, by the dose or concentration of drug, D; D_m is the dose required to produce the median–effect (i.e. 50% affected or in the present case 50% inhibition of cell growth or IC_{50}); and m is a Hill-type coefficient signifying the sigmoidicity of the dose–effect curve. Since by definition, $f_a + f_u = 1$, several useful alternative forms of Equation 1 are possible, one of which being:

$$[(f_a)^{-1} - 1]^{-1} = \left[\frac{D}{D_m}\right]^m \tag{2}$$

which can be linearized by taking logarithms of both sides:

$$\log[(f_a)^{-1} - 1]^{-1} = m\log(D) - m\log(D_m). \tag{3}$$

Equation 3 forms the basis for the median–effect plot (see Fig. 1) where the slope of the lines is equal to m and the x-intercept, $\log D_m$. The D_m can be calculated from the antilog of $-(\text{y intercept})/m$.

The median–effect principle has been extended to multiple drug effects. For the summation of effect of two drugs (see Ref. 11 for derivation):

$$\left[\frac{(f_a)_{1,2}}{(f_u)_{1,2}}\right]^{1/m} = \left[\frac{(f_a)_1}{(f_u)_1}\right]^{1/m} + \left[\frac{(f_a)_2}{(f_u)_2}\right]^{1/m} + \left[\frac{\alpha(f_a)_1(f_a)_2}{(f_u)_1(f_u)_2}\right]^{1/m} = \frac{(D)_1}{(D_m)_1} + \frac{(D)_2}{(D_m)_2} + \frac{\alpha(D)_1(D)_2}{(D_m)_1(D_m)_2}. \tag{4}$$

For mutually exclusive drugs, $\alpha = 0$ and the median–effect plot gives parallel lines for the parent drugs and their mixture ($m_1 = m_2 = m_{1,2}$). When $\alpha = 1$, the effects of the two drugs are mutually nonexclusive and the median–effect plots produce lines where $m_1 = m_2 < m_{1,2}$. The interaction of two drugs can be quantitated as a "combination index" or *CI* where:

$$CI = \frac{(D)_1}{(D_x)_1} + \frac{(D)_2}{(D_x)_2} + \frac{\alpha(D)_1(D)_2}{(D_x)_1(D_x)_2} \tag{5}$$

where D_x is the dose that is required to produce x% affected. Sets of D_x and x% can be calculated from equation 1 by knowing D_m and m obtained from the median–effect plot. A plot can be generated depicting *CI* at various fractions affected as in Fig. 2. When $CI = 1$ or < 1 or > 1, then summation or synergism or antagonism is indicated.

DNA strand scission. DNA single-strand breaks were measured by alkaline elution as described by Kohn *et al.* [13]. L1210 cells in early log growth were grown in 1 μM [*methyl*-^{14}C]thymidine, at a specific activity of 0.02 μCi/nmol, or 1 μM [*methyl*-^{3}H]thymidine, at 0.1 μCi/nmol, for 24 hr. The [^{14}C]thymidine-labeled cells were exposed to drug at a specified concentration and time interval, after which 5×10^5 cells were mixed with an equal number of [^{3}H]thymidine-labeled cells which had been X-irradiated previously with 300 rads as an internal standard. The cells were placed on polycarbonate filters (2 μm pore diameter; Nucleopore Corp., Pleasanton, CA) in a 25-mm filter holder with a 50-mL funnel (Millipore, Bedford, MA) and washed by gravity with three 5-mL aliquots of ice-cold phosphate-buffered saline. The cells were lysed by passing 5 mL of 2% sodium dodecyl sulfate/25 mM EDTA, pH 9.7, through the filter. Two milliliters of the same solution containing 0.5 mg of proteinase K/mL (Sigma) were layered over the cells and pumped through the filter at 20 μL/min for 1 hr, collecting the eluate into scintillation vials. The funnel was then filled with eluting buffer (tetrapropylammonium hydroxide/25 mM EDTA/0.1% sodium dodecyl sulfate, pH 12.1), and this solution was pumped through the filter at 20 μL/min with 1-hr fractions being collected for at least 16 hr. At the end of the run the filters were placed in scintillation vials and incubated with 0.4 mL of 1 N HCl at 60° for 1 hr, followed by 1 mL of 1 N NaOH for 1 hr at room temperature. Residual radioactivity in the filter holders and tubing was pumped into scintillation vials with an additional 2 mL of eluting buffer. All radioactivity was incorporated into Ready-Solv (Beckman) containing 0.7% acetic acid. Counting efficiencies were determined with [^{14}C] and [^{3}H] standards (Amersham), and radioactivity contributed by each isotope was determined by the method of dual channel counting. Data were graphed as a log-log plot of [^{14}C] versus [^{3}H] retained on the filter, and single-strand break frequency, expressed as rad equivalents, was calculated as previously described [13]. Repair of single-strand breaks was assessed by first incubating cells with drug for 1 hr, washing the cells twice in an excess of medium, and resuspending the cells into 10 mL of medium at 37°. Cells were then incubated at 37°, and aliquots (10^6 cells) were periodically removed and lysed on filters following the procedure for single-strand breaks.

Those procedures requiring X-irradiated cells employed a 120 kV, 5 milliamp X-ray tube (Torr X-

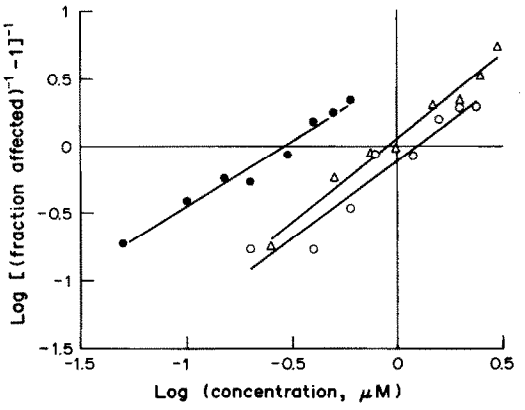

Fig. 1. Median–effect plot [11, 12] for the inhibition of L1210 outgrowth by trimetrexate, etoposide or their combination. Cells were exposed to drug for 2 hr, and the ratio of etoposide to trimetrexate was held constant at 4 throughout the concentration range. See Methods for additional details on the median–effect plot. Key: (●) trimetrexate, (○) etoposide, and (△) trimetrexate + etoposide.

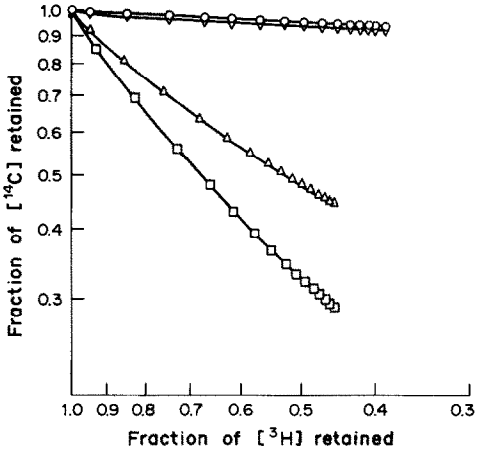

Fig. 3. Alkaline elution profile showing DNA single-strand breaks caused by etoposide, trimetrexate or their combination in L1210 cells. Cells were exposed to 0.5 μM drug for 2 hr. Experimental details are given in Methods. Key: (○) untreated control, (◇) trimetrexate, (△) etoposide, and (□) trimetrexate + etoposide.

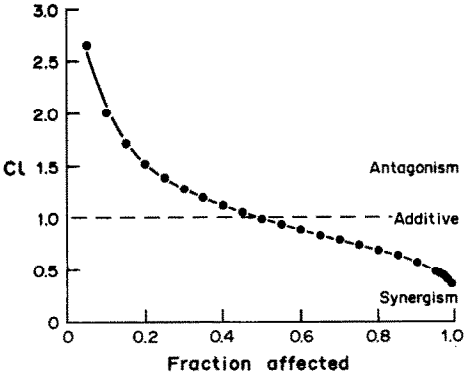

Fig. 2. Computer-generated graphical presentation showing interactions between trimetrexate and etoposide. *CI* represents the combination index [11, 12]. See Methods for details of this plot.

ray, Burlington, MA) set in a self-contained lead-lined cabinet (Test Equipment Distributors, Troy, MI). Cells were kept on ice during and after irradiation until they were lysed on the filters. Radiation doses were monitored with a model 500 dual polarity electrometer, equipped with a 0.33-cc probe (Victoreen Inc., Cleveland, OH).

Transport of etoposide. Transport studies were conducted in RPMI medium plus 10% fetal calf serum identical to that employed for the synergy and DNA strand break experiments. L1210 cells were grown to approximately 5×10^5/mL, collected by centrifugation, and resuspended into fresh medium at 1×10^7/mL. Cells were agitated with a shaking water bath and maintained in an atmosphere containing 5% CO_2 in air. Fluxes were initiated by exposing the cells to 0.5 μM tritiated etoposide (final specific activity, 1 μCi/nmol) with or without 0.5 μM trimetrexate. Transport was abolished at designated internals by injecting 1 mL of cell suspension into 10 vol. of ice-cold phosphate-buffered saline (PBS). The cells were washed twice by centrifugation with 5 mL of ice-cold PBS, and the pellet was digested in 1 mL Protosol (New England Nuclear, Boston, MA). Radioactivity was determined in a Beckman model 6800 liquid scintillation counter, and counting efficiencies were determined with quenched standards.

Ribonucleoside triphosphate analysis. Approximately 10^7 cells were extracted with 0.5 mL of 0.7 N perchloric acid. Extracts were centrifuged to remove precipitated protein, neutralized with solid potassium bicarbonate, and centrifuged once more to remove potassium perchlorate. Then 50 μL of the supernatant was analyzed by anion-exchange chromatography in a Perkin–Elmer series 4 liquid chromatograph equipped with a Whatman Pellicular anion exchange precolumn (0.4 × 6 cm) and a Whatman Partisil PSX 10/25 SAX column (0.46 × 25 cm). Nucleosides were resolved with an ammonium phosphate gradient starting with 5 mM, pH 2.8, and ending at 0.5 M, pH 4.8. Precise details of the elution procedure are given elsewhere [14]. Peaks were detected using a Kratos spectroflow UV detector and integrated with a Perkin–Elmer Sigma 15 integrator calibrated against known standards.

RESULTS

Combination of trimetrexate and etoposide on cell growth. Figure 1 represents a median–effect plot [11, 12] and illustrates the outgrowth inhibition of L1210 cells by trimetrexate, etoposide and their combination. The ratio of the two drugs was held constant at 4 to 1 (etoposide to trimetrexate), and the linearity of the plots ($r = 0.97$, 0.92 and 0.98 for trimetrexate, etoposide and their combination, respectively) illustrates the applicability of the median–effect method.

Table 1. Effect of trimetrexate on the repair of protein-associated DNA strand breaks in L1210 cells exposed to etoposide

Treatment during initial incubation*	Treatment during repair period	% Repair†	
		30 min	60 min
0.5 μM Etoposide	None	69	92
0.5 μM Etoposide + 0.5 μM trimetrexate	None	70	96
0.5 μM Etoposide + 0.5 μM trimetrexate	0.5 μM Trimetrexate	66	88

* The initial incubation period was 2 hr.

† DNA damage and repair were assessed by alkaline elution. Percent repair represents the percentage decrease in the net slope generated by plotting [^{14}C] remaining on the filter from treated cells versus [^{3}H] from irradiated control cells.

The slopes of the lines (m) were 0.98, 1.16 and 1.26, respectively, and therefore not parallel which suggests that trimetrexate and etoposide may be mutually nonexclusive drugs. A computer-generated graphical presentation (Fig. 2) of the combination index (CI) with respect to the fraction affected was derived with parameters obtained from Fig. 1. CI in this case was calculated from Equation 5 (Methods) where $\alpha = 1$. This plot indicates that a combination of the two drugs will produce a synergistic effect but only at concentrations of drugs that affect greater than 50% of the cells. A plot based on CI values calculated from Equation 5 where $\alpha = 0$ also showed synergy at the higher doses (data not shown). Based on this information, the subsequently described mechanistic studies designed to investigate the mechanism of synergy between trimetrexate and etoposide were performed at drug combinations that would reduce growth by at least 90% after a 2-hr exposure.

Effect of trimetrexate on etoposide-mediated protein-associated DNA strand breaks. Since recent evidence suggests that the mechanism of cytotoxicity for etoposide is topoisomerase II-mediated DNA strand breaks [9], the production of these lesions was assessed in the presence of etoposide alone and in combination with trimetrexate. Figure 3 shows an alkaline elution profile demonstrating DNA single-strand breaks in L1210 cells exposed for 2 hr to either 0.5 μM etoposide, trimetrexate or their combination. Although trimetrexate by itself caused no DNA breaks under these conditions, its combination with etoposide significantly increased the elution rate over etoposide alone. These data were converted to X-ray rad equivalents [13] for a more quantitative comparison. Trimetrexate, etoposide or their combination caused 2, 455 and 788 rad equivalents, respectively, under the conditions described for Fig. 3. This indicates that the combination of trimetrexate with etoposide produced an additional 333 rad equivalents. These additional DNA strand breaks appear to be protein-associated, similar to those caused by etoposide alone, since in the absence of treating the cell lysate with proteinase, no increase in elution rates were observed in cells exposed to the drugs singly or in combination (data not shown).

In an effort to find out why trimetrexate potentiated the DNA strand breaks produced by etoposide, its effect was determined on several biochemical and pharmacological parameters of etoposide. The effect of trimetrexate on the net transport of etoposide was assessed under the same conditions and at drug concentrations which potentiated DNA damage. No significant difference in initial rate or intracellular levels at the steady state

Table 2. Effect of trimetrexate with or without various potential protectants on ribonucleoside triphosphate pools and DNA single-strand breaks produced by etoposide in L1210 cells

Addition*	Etoposide* (μM)	Trimetrexate* (μM)	ATP†	GTP	CTP	UTP	SSB‡ (rads)
Control	0	0	2638 ± 179	602 ± 32	459 ± 47	1398 ± 98	
None	0.5	0	98	101	95	102	498 ± 49
None	0.5	0.5	46	22	151	240	728 ± 56
100 μM Hypoxanthine	0.5	0.5	112	100	69	58	468 ± 22
10 μM Thymidine	0.5	0.5	45	24	131	209	718 ± 42
100 μM Guanosine	0.5	0.5	40	498	56	60	699 ± 67
20 μM Adenosine	0.5	0.5	142	108	75	74	456 ± 82
100 μM Cytidine	0.5	0.5	36	22	180	195	721 ± 43
100 μM Uridine	0.5	0.5	39	22	135	226	734 ± 71

* Cells were exposed to the indicated concentrations of drugs for 2 hr.

† Ribonucleotides for the control cells are expressed as pmol/10^6 cells (mean ± SE). Values from treated cells represent the percent of each respective control. All results are the mean of three experiments.

‡ DNA strand breaks, expressed as X-ray rad equivalents, were determined by alkaline elution as described in Methods. Values are means ± SE, N = 3.

Table 3. Effects of various antimetabolites on ribonucleoside triphosphate pools and DNA single-strand breaks produced by etoposide in L1210 cells

Additions*	Etoposide* (μM)	ATP†	GTP	CTP	UTP	SSB‡ (rads)
Control	0	2650 ± 252	605 ± 41	425 ± 43	1360 ± 132	
None	0.5	94	96	99	98	498 ± 49
0.5 μM Trimetrexate	0.5	41	21	136	212	728 ± 56
0.5 μM Methotrexate	0.5	42	30	116	149	730 ± 41
0.5 μM 5,10-Dideazatetrahydrofolate	0.5	48	54	111	139	602 ± 32
20 μM CB-3717	0.5	109	113	108	116	463 ± 59
1 μM Pyrazofurin	0.5	142	173	36	24	485 ± 36
0.5 μM Trimetrexate + 1 μm pyrazofurin	0.5	34	25	30	40	734 ± 42

* Cells were exposed to the indicated concentrations of drugs for 2 hr.

† Ribonucleotides for the control cells are expressed as pmol/10^6 cells (mean ± SE). Values from treated cells represent the percent of each respective control. All results are the mean of three experiments.

‡ DNA strand breaks, expressed as X-ray rad equivalents, were determined by alkaline elution as described in Methods. Values are means ± SE, N = 3.

were observed between control and trimetrexate-treated cells. These results were not biased by changes in cell volume since there was no significant change in intracellular water under each condition (data not shown). Another possible explanation is that trimetrexate does not potentiate the DNA strand breaks produced by etoposide but slows any repair of these lesions that might occur during the drug treatment period. Table 1 shows experimental data related to this possibility. Cells were exposed to 0.5 μM etoposide with or without 0.5 μM trimetrexate. After 2 hr the drug(s) was removed by washing the cells in medium and the repair period was initiated by resuspending into 37° medium with or without trimetrexate. After 0, 30 and 60 min of repair, alkaline elution was performed to assess remaining DNA strand breaks. No significant reduction in extent of repair was observed under any of the described conditions.

Effects of nucleotide protectants on the potentiation of etoposide-mediated DNA strand breaks by trimetrexate and their effect on ribonucleoside triphosphate pools. One of the better known biochemical responses in cells exposed to trimetrexate is a reduction in purine ribonucleotide pools [3]. To assess whether these perturbations may be related to the increase in strand breaks produced by etoposide, DNA single-strand breaks and ribonucleoside triphosphate pools were measured in L1210 cells exposed to combinations of trimetrexate and etoposide with or without various nucleoside protectants. Table 2 shows that etoposide alone had no effect on ribonucleoside triphosphate pools whereas added trimetrexate produced the usual increase in DNA single-strand breaks as well as a 54 and 78% depletion of ATP and GTP, respectively, and an elevation in pyrimidine nucleotides. The addition of hypoxanthine or adenosine restored purine intracellular concentrations to control values and also prevented the increase in DNA strand breaks. Thymidine, cytidine and uridine elevated pyrimidine levels but with no effect on augmentation of the strand breaks. Addition of guanosine elevated GTP but not the ATP and under these conditions there was the full augmentation of strand breaks. Thus, only those protectants that restored ATP pools were able to prevent the increase in DNA damage.

Effects of other inhibitors of the purine or pyrimidine pathways on etoposide-mediated DNA strand breaks. Similar to trimetrexate, the antifolate methotrexate reduced purine nucleotides and also potentiated etoposide-mediated strand breaks (Table 3). Inhibitors of dihydrofolate reductase, however, not only reduce purines but also deplete thymidylate pools. To further distinguish between purine and pyrimidine effects on etoposide action, several other agents which more specifically perturb nucleotide metabolism were combined with etoposide. Cells were exposed to 5,10-dideazatetrahydrofolate (DDTHF) which has been reported to be a specific inhibitor of glycinamide adenine ribonucleotide transformylase [15], an enzyme which occupies an integral position in the *de novo* purine biosynthetic pathway. Purine nucleotides were reduced in the presence of this agent and again there was a stimulation of etoposide-mediated DNA single-strand breaks (Table 3). In contrast, when etoposide was combined with CB-3717, a quinazoline which selectively depletes thymidylate pools by inhibition of thymidylate synthase [16], there was no potentiation of DNA strand breaks nor depletion of purine nucleotides. To ensure that there was no involvement of the pyrimidine pools, etoposide was combined with pyrazofurin, an agent that inhibits orotidylate decarboxylase and depletes pyrimidines [17]. Table 3 shows that pyrazofurin caused a severe reduction in CTP and UTP but had no effect on single-strand breaks produced by etoposide. When all ribonucleotides were depleted by a combination of pyrazofurin and trimetrexate, no greater or lesser augmentation of etoposide effects were produced than with the etoposide–trimetrexate combination alone.

Relationship between intracellular ATP concentration and the number of DNA strand breaks produced by etoposide. The data thus far indicate a strong relationship between the decline in ATP levels produced by trimetrexate or other inhibitors of the purine pathway and the augmentation of etoposide-mediated strand breaks. This relationship was investigated further by exposing cells to a combination of

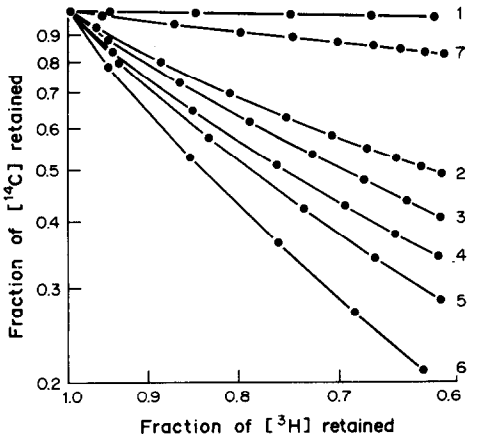

Fig. 4. Alkaline elution profile showing the effect of 2,4-dinitrophenol on DNA single-strand breaks produced by etoposide in L1210 cells. Cells were exposed to the following for 2 hr: (1) untreated control. (2) 0.5 μM etoposide, (3) 0.5 μM etoposide + 25 μM DNP, (4) 0.5 μM etoposide + 50 μM DNP, (5) 0.5 μM etoposide + 100 μM DNP, (6) 0.5 μM etoposide + 150 μM DNP, and (7) 0.5 μM etoposide + 150 μM DNP + 20 mM 2-deoxyglucose.

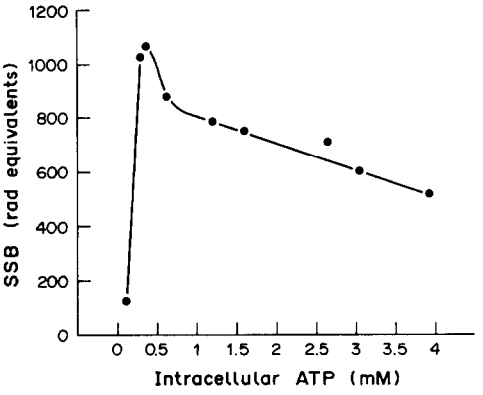

Fig. 5. Relationship between intracellular ATP concentrations and number of DNA single-strand breaks produced by etoposide in L1210 cells. Cells were exposed to 0.5 μM etoposide plus various concentrations of DNP (listed in Table 5) for 2 hr and then subjected to nucleotide analysis and alkaline elutions as described in Methods.

etoposide and various concentrations of 2,4-dinitrophenol (DNP), an uncoupler of oxidative phosphorylation. Figure 4 shows an alkaline elution profile for L1210 cells exposed to 0.5 μM etoposide with or without various concentrations of DNP for 2 hr. Elution rates were directly proportional to the concentration of DNP. If the highest concentration of DNP (150 μM) was combined with 20 mM 2-deoxyglucose, an inhibitor of the glycolytic pathway, the elution rate returned to approximately the control. A 2-hr exposure to 20 mM 2-deoxyglucose alone depressed ATP levels in L1210 cells by ~35% and resulted in a 27% increase in DNA single-strand breaks. DNP and/or 2-deoxyglucose without etoposide had no effect on elution rate (data not shown). ATP levels were measured in cells under identical conditions as those in Fig. 4 and are listed in Table 4 along with the associated single-strand break rad equivalents. There was an inverse relationship between intracellular ATP levels and etoposide-mediated DNA strand breaks until the nucleotide concentration dropped below 180 pmol/10^6 cells, whereby there was a precipitous drop in DNA single-strand breaks. This relationship is expressed graphically in Fig. 5 where ATP levels have been converted to millimolar concentrations based on intracellular water content of 0.52 μL/10^6 cells.

DISCUSSION

A number of previous studies have reported either therapeutic synergism or enhancement of DNA strand breaks when inhibitors of topoisomerase were combined with certain antimetabolites [18, 19]. These combinations include 1-β-D-arabinofuranosylcytosine or hydroxyurea with amsacrine [20], methotrexate and teniposide [21], methotrexate and etoposide [22], and 5-azacytidine and amsacrine [23]. Other agents that have been shown to modulate inhibitors of topisomerase are α-difluoromethylornithine [24–26], 4-hydroperoxycyclophosphamide [27], cisplatin [28] and 17-β-estradiol in estrogen receptor positive breast tumors [29, 30]. Several explanations for these interactions have been put forth which include cell synchronization, modification of DNA chromatin structure, or inhibition of DNA repair.

The present study demonstrates cytotoxic synergy *in vitro* in L1210 cells exposed to combinations of etoposide and trimetrexate and provides evidence to suggest a specific biochemical mechanism. Trimetrexate produced an increase in DNA strand breaks caused by etoposide, and the experimental results clearly imply that a reduction in intracellular ATP levels contributed significantly to this result. This conclusion is supported by three lines of evidence: (1) only those antimetabolites that reduced purine nucleotides were capable of increasing etoposide-mediated DNA damage, whereas drugs that perturb pyrimidine pools had no effect; (2) only nucleosides that restored ATP levels, such as hypoxanthine or adenosine, were capable of preventing the augmentation of DNA damage by trimetrexate; and (3) the number of DNA strand breaks produced by etoposide was inversely proportional to intracellular ATP levels when reduced by various concentrations of 2,4-dinitrophenol. The observation that synergy occurred only at more cytotoxic concentrations of trimetrexate may reflect the fact that purine nucleotide pools are not depressed enough at low drug concentrations to cause a significant effect.

Two other possible explanations for the observed effects on etoposide action have been ruled out. Trimetrexate had no effect on transport of etoposide under identical conditions where synergy was observed nor was there any effect of trimetrexate on the repair of etoposide-mediated DNA strand breaks. Another explanation that has been offered in the literature [22] for synergistic interaction of antimetabolites and DNA damaging agents is cell

Table 4. Effect of 2,4-dinitrophenol on intracellular ATP concentrations and protein-associated strand breaks produced by etoposide in L1210 cells*

2,4-Dinitrophenol (μM)	ATP (pmol/10^6 cells)	Single-strand breaks (rad equivalents)
—	2034 ± 181	519 ± 19
25	1583 ± 154	604 ± 62
50	1372 ± 205	710 ± 55
75	825 ± 56	750 ± 69
100	625 ± 51	785 ± 71
125	321 ± 27	878 ± 85
150	183 ± 22	1068 ± 79
200	150 ± 12	1027 ± 72
200 + 20 mM 2-Deoxyglucose	61 ± 11	125 ± 22

* Cells were incubated with 0.5 μM etoposide plus the indicated concentrations of dinitrophenol for 2 hr and then subjected to either nucleotide analysis or alkaline elution as described in Methods. Each value is the mean ± SE of three experiments.

synchronization by the first drug which then allows most cells to enter the S phase simultaneously, thus making the majority susceptible to the second drug. This possibility is unlikely, however, since the experiments in the present study were short term, lasting only 2 hr which is not enough time for cells to accumulate significantly in any part of the cell cycle.

Another study which addresses the relationship between ATP and topoisomerase-mediated cytotoxicity was reported by Kupfer *et al.* [31] in which a reduction in the cytotoxicity of teniposide was observed in the presence of DNP or other metabolic inhibitors. This study seemingly contradicts the present results since no synergy was observed. However, in the former study, the concentration of epipodopholotoxin was 10 μM teniposide versus the 0.5 μM etoposide used in the present study. This not only represents a 20-fold difference in concentration but since teniposide is 10-fold more potent than etoposide, both in cytotoxicity and production of protein-associated strand breaks, it represents a 200-fold increase in DNA strand-breaking capacity. It may be that, at these superlethal concentrations of drug, the production of protein-associated DNA strand breaks is rapid enough to change drastically the ATP requirements of topoisomerase II.

Modulation of etoposide-mediated DNA strand breaks by ATP is not an unreasonable concept since topoisomerase II is an ATP-requiring enzyme. However, since there is an inverse relationship between ATP and activity, it appears that under normal conditions the enzyme must be under some degree of substrate inhibition at least with regard to formation of etoposide-induced cleavable complexes. Based on the present data, it appears to be operating at about 50% of its maximum since peak stimulation was about 2-fold. From nucleotide analysis and intracellular water values, estimates of intracellular ATP concentration in control cells were between 3 and 4 mM. The hypothesis that cleavable complex formation by etoposide would be partially suppressed under this concentration of ATP is supported by studies with isolated nuclei from L1210 cells where concentrations of ATP in excess of 1 mM inhibit etoposide-induced strand breaks [32]. Similar observations have also been reported in isolated nuclei from K562 human leukemia cells [33]. In the present study, the production of DNA strand breaks by etoposide appears to peak at ATP levels of between 180 and 320 pmol/10^6 cells which corresponds roughly to 350–600 μM. Below these levels, production of strand breaks declined and presumably ATP concentrations became rate limiting. A reduction in enzyme activity as ATP levels decrease through this range of concentrations is consistent with known kinetic properties of topoisomerase II which reportedly has a K_m for ATP of around 200 μM [34].

REFERENCES

1. Elslager EF and Davoll J, Synthesis of fused pyrimidines as folate antagonists. In: *Lectures in Heterocyclic Chemistry* (Eds. Castle RN and Townsend LB), pp. S.97–S.133. Tetero Corp., Orem, UT, 1974.
2. Elslager EF, Johnson JL and Werbel LM, Folate antagonists. 20. Synthesis and antitumor and antimalarial properties of trimetrexate and related 6-[(phenylamino)methyl]-2,4-quinazolinediamines. *J Med Chem* **26**: 1753–1760, 1983.
3. Jackson RC, Fry DW, Boritzki TJ, Besserer J, Leopold WR, Sloan BJ and Elslager EF, Biochemical pharmacology of the lipophilic antifolate, trimetrexate. *Adv Enzyme Regul* **22**: 187–206, 1984.
4. Lin JT and Bertino JR, Trimetrexate: A second generation folate antgonist in clinical trial. *J Clin Oncol* **5**: 2032–2040, 1987.
5. Issel BF, The podophyllotoxin derivatives VP16-213 and VM26. *Cancer Chemother Pharmacol* **7**: 73–80, 1982.
6. Issell BF, Rudolph AR and Louie AC, Etoposide (VP-16-213): An overview. In: *Etoposide (VP-16): Current Status and New Developments* (Eds. Issell BF, Muggia FM and Carter SK), pp. 1–14. Academic Press, New York, 1984.
7. Bunn PA, The role of chemotherapy in small-cell lung cancer. In: *Etoposide (VP-16): Current Status and New Developments* (Eds. Issell BF, Muggia FM and Carter SK), pp. 141–161. Academic Press, New York, 1984.
8. Williams SD, Birch R, Loehrer PJ and Einhorn LH, Testicular cancer: Role in chemotherapy. In: *Etoposide*

(VP-16): Current Status and New Developments (Eds. Issell BF, Muggia FM and Carter SK), pp. 225–232. Academic Press, New York, 1984.
9. Clark PI and Slevin ML, The clinical pharmacology of etoposide and teniposide. *Clin Pharmacokinet* **12**: 223–252, 1987.
10. Rottenberg H, The measurement of membrane potential and ΔpH in cells, organelles, and vesicles. *Methods Enzymol* **55**: 547–569, 1979.
11. Chou T-C and Talalay P, Quantitative analysis of dose–effect relationships: The combined effects of multiple drugs or enzyme inhibitors. In: *Advances in Enzyme Regulation* (Eds. Weber G), pp. 27–55. Pergamon Press, New York, 1984.
12. Chou T-C and Talalay P, Applications of the median–effect principle for the assessment of low-dose risk of carcinogens and for the quantitation of synergism and antagonism of chemotherapeutic agents. In: *New Avenues in Developmental Cancer Chemotherapy* (Eds. Harrap KR and Connors TA), pp. 37–64. Academic Press, New York, 1987.
13. Kohn KW, Ewig RAG, Erickson LC and Zwelling LA, Measurement of strand breaks and cross-links by alkaline elution. In: *DNA Repair. A Laboratory Manual of Research Procedures* (Eds. Friedberg EC and Hanawalt PC), pp. 379–401. Marcel Dekker, New York, 1981.
14. Fry DW, Boritzki TJ, Besserer JA and Jackson RC, *In vitro* DNA strand scission and inhibition of nucleic acid synthesis in L1210 leukemia cells by a new class of DNA complexers, the anthra[1,9-*cd*]pyrazol-6(2*H*)-ones (anthrapyrazoles). *Biochem Pharmacol* **34**: 3499–3508, 1985.
15. Beardsley GP, Moroson BA, Taylor EC and Moran RG, A new folate antimetabolite, 5,10-dideaza-5,6,7,8-tetrahydrofolate is a potent inhibitor of *de novo* purine synthesis. *J Biol Chem* **264**: 328–333, 1989.
16. Jackson RC, Jackman AL and Calvert AH, Biochemical effects of a quinazoline inhibitor of thymidylate synthetase, *N*-(4-(*N*-((2-amino-4-hydroxy 6-quinazolinyl)methyl)prop - 2 - ynylamino)benzoyl) - L-glutamic acid (CB3717), on human lymphoblastoid cells. *Biochem Pharmacol* **32**: 3783–3790, 1983.
17. Cadman EC, Dix DE and Handschumacher RE, Clinical, biological, and biochemical effects of pyrazofurin. *Cancer Res* **38**: 682–688, 1978.
18. Zwelling LA, Silberman L and Estey E, Biochemical basis for tumoricidal synergism between antimetabolites and DNA intercalating agents. *Cancer Bull* **37**: 187–192, 1985.
19. Zwelling LA, Silberman L and Estey E, Intercalator-induced, topoisomerase II-mediated DNA cleavage and its modification by antineoplastic antimetabolites. *Int J Radiat Oncol Biol Phys* **12**: 1041–1047, 1986.
20. Minford J, Kerrigan D, Nichols M, Shackney S and Zwelling LA, Enhancement of the DNA breakage and cytotoxic effects of intercalating agents by treatment with sublethal doses of 1-β-D-arabinofuranosylcytosine or hydroxyurea in L1210 cells. *Cancer Res* **44**: 5583–5593, 1984.
21. Wampler GL, Carter WH, Campbell ED and Goldman ID, Demonstration of a schedule-dependent therapeutic synergism utilizing the interacting drugs methotrexate and teniposide in L1210 leukemia. *Cancer Treat Rep* **71**: 581–591, 1987.
22. Lorico A, Rappa G, Boiocchi M, Anaznello F and D'Incalci M, Increase in etoposide-induced topoisomerase II-mediated DNA breaks after cell synchronization induced by low doses of methotrexate. *Biochem Pharmacol* **37**: 1883–1884, 1988.
23. Zwelling LA, Minford J, Nichols M, Glazer RI and Shackney S, Enhancement of intercalator-induced DNA scission and cytotoxicity in murine leukemia cells treated with 5-azacytidine. *Biochem Pharmacol* **33**: 3903–3906, 1984.
24. Bakic M, Chan D, Freireich EJ, Marton LJ and Zwelling LA, Effect of polyamine depletion by α-difluoromethylornithine or (2*R*,5*R*)-6-heptyne-2,5-diamine on drug-induced topoisomerase II-mediated DNA cleavage and cytotoxicity in human and murine leukemia cells. *Cancer Res* **47**: 6437–6443, 1987.
25. Zwelling LA, Kerrigan D and Marton LJ, Effect of difluoromethylornithine, an inhibitor of polyamine biosynthesis, on the topoisomerase II-mediated DNA scission produced by 4′-(9-acridinylamino)methane sulfon-*m*-anisidide in L1210 murine leukemia cells. *Cancer Res* **45**: 1122–1126, 1985.
26. Dorr RT, Liddil JD and Gerner EW, Modulation of etoposide cytotoxicity and DNA strand scission in L1210 and 8226 cells by polyamines. *Cancer Res* **46**: 3891–3895, 1986.
27. Chang TT, Gulati SC, Chou T-C, Vega R, Gandola L, Ezzat Ibrahim SM, Yopp J, Colvin M and Clarkson BD, Synergistic effect of 4-hydroperoxycyclophosphamide and etoposide on a human promyelocytic leukemia cell line (HL-60) demonstrated by computer analysis. *Cancer Res* **45**: 2434–2439, 1985.
28. Durand RE and Goldie JH, Interaction of etoposide and cisplatin in an *in vitro* tumor model. *Cancer Treat Rep* **71**: 673–679, 1987.
29. Zwelling LA, Kerrigan D and Lippman ME, Protein-associated intercalator-induced DNA scission is enhanced by estrogen stimulation in human breast cancer cells. *Proc Natl Acad Sci USA* **80**: 6182–6186, 1983.
30. Epstein RJ and Smith PJ, Estrogen-induced potentiation of DNA damage and cytotoxicity in human breast cancer cells treated with topoisomerase II-interactive antitumor drugs. *Cancer Res* **48**: 297–303, 1988.
31. Kupfer G, Bodley AL and Liu LF, Involvement of intracellular ATP in cytotoxicity of topoisomerase II-targeting antitumor drugs. In: *NCI Monographs. First Conference on DNA Topoisomerases* (Eds. Potmesil M and Ross WR), pp. 37–40. U.S. Government Printing Offices, Washington, DC, 1987.
32. Glisson BS, Smallwood SE and Ross WE, Characterization of VP-16-induced DNA damage in isolated nuclei from L1210 cells. *Biochim Biophys Acta* **783**: 74–79, 1984.
33. Yalowich JC and Benton S, Effects of nucleotides on VP-16-induced DNA damage in nuclei from human leukemia K562 cells sensitive and resistant to VP-16. *Proc Am Assoc Cancer Res* **29**: 1261, 1988.
34. Halligan BD, Edwards KA and Liu LF, Purification and characterization of a type II DNA topoisomerase from bovine calf thymus. *J Biol Chem* **260**: 2475–2482, 1985.